MODELING THE DYNAMIC BEHAVIOR OF ESTROGEN DOCKING INTO ITS RECEPTOR USING THE MULTISCALE ANALYSIS.

by

ANUDEEP PALANKI

Presented to the Faculty of the Graduate School of
The University of Texas at Arlington in Partial Fulfillment
of the Requirements
for the Degree of

MASTER OF SCIENCE IN MECHANICAL ENGINEERING

THE UNIVERSITY OF TEXAS AT ARLINGTON

May 2013

To my Mother, Sujata, Father, Rama Rao, Brother, Ratan and Gradmother, Indira, whose support, guidance and motivation made made me who I am.

ACKNOWLEDGEMENTS

I would like to thank my supervising professor Dr. Alan Bowling for constantly motivating and encouraging me, and also for his invaluable advice during the course of my Master's studies. I wish to thank my academic advisor Dr. Siechii Nomura. I would also like to extend my gratitude to Dr. Peter Kroll and Dr. Subhrangsu Mandal, Department of Chemistry and Biochemistry, UTA for their valuable suggestions. I would also like to thank Dr. Adnan Ashfaq and Dr. Hyejin Moon for their interest in my research and for taking time to serve in my thesis committee.

I would also like to thank Dr.Bernd Chudoba, for his invaluable guidance during my brief time in his lab. I would also like to extend my Gratitude to Dr.Kamesh Subbarao, for his valuable inputs.

I wish to thank my Lab mates, Mahdi Haghshenas-Jaryani for his thoughtful suggestions and Adrian Rodriguez, Zachary Brush, Sarvenaz Ghaffari for their inputs.

April 22, 2013

ABSTRACT

MODELING THE DYNAMIC BEHAVIOR OF ESTROGEN DOCKING INTO ITS RECEPTOR USING THE MULTISCALE ANALYSIS.

Anudeep Palanki, M.S.

The University of Texas at Arlington, 2013

Supervising Professor: Alan Bowling

This work models the dynamic behavior of Estrogen docking into its receptor. It lays the foundation for the development of a new theoretical screening technique to identify carcinogens. It is predicted that this year, more than 1 million Americans and more than 10 million people worldwide will be diagnosed with cancer. Only 5 to 10 percent of all cancer cases can be attributed to genetic defects, whereas the remaining 90 to 95 percent have their roots in the environment. It has been suggested that some chemical compounds have a similar structure and properties as natural hormones produced by the human body. Hence they can trigger the release of growth hormones that lead to unnatural tissue growth, and ultimately the tumors, indicative of cancer.

This first generation work is aimed at developing a technique to screen the environmental chemicals that cause breast cancer and hence the natural hormone of interest is Estrogen. In this work, the 2 dimensional coarse grained model of estrogen is described, along with its advantages over the current theoretical approaches. Then, the dynamic model of the estrogen is presented explaining the various forces that

act on the system. Then, the simulation results of the docking are discussed for various boundary conditions highlighting the importance of the Estrogen Receptor in the docking process. Finally, the multi scale analysis is performed on the system accurately predicting the dynamics of the system while achieving *drastic* reductions in CPU run time. Then, this work is concluded expressing the future scope for this project.

TABLE OF CONTENTS

ACKNOWLEDGEMENTS iv

ABSTRACT v

LIST OF ILLUSTRATIONS ix

LIST OF TABLES xi

Chapter Page

1. Introduction 1

2. Background 4

3. Method Implemented 9

3.1 Rigid multibody model 9

3.2 Multi Scale Analysis 13

3.3 Mass and Inertia Calculation 16

3.4 Viscous Forces 17

3.5 Charge Forces 19

3.6 Brownian Motion 23

4. Results and Discussion 25

5. Conclusion 34

Appendix

A. Locations of bodies and points 35

B. Inertia Calculations 39

C. Drag Forces 42

D. Brownian Motion 44

REFERENCES 46

BIOGRAPHICAL STATEMENT 53

LIST OF ILLUSTRATIONS

Figure		Page
1.1	Estrogen Receptor, 17β-Estradiol and Xenoestrogens	2
2.1	Xenoestrogen Examples [7]	4
3.1	Figure showing the estrogen docked in the receptor as revelaed from the diffraction studies and the coarse grained model used in this work. . .	10
3.2	Figure shows the axis used to calculate the inertias for bodies	16
3.3	Drag forces on Estrogen	18
3.4	Figure showing the forces due to hydrogen bonds.	20
3.5	Graph of Interaction Potential vs Distance	22
3.6	Brownian Motion acting on Estrogen	23
4.1	Simulation of Estrogen docking into its receptor, $q_1 = 30$, $q_2 = 20$, Rel Error = 10^{-8} and Abs Error = 10^{-7}, CPU run time = 20 mins	25
4.2	Graphs showing the Charge Potential and Force Vs Distance for one of the charges. The points A, B, C and D indicate various significant values during the docking.	26
4.3	Figure shows the graph of q_1 Vs time with and without the brownian force and the hydrophobic bonds formed by docked Estrogen.	27
4.4	The plot of Force Vs Time, $q_1 = 30$, $q_2 = 20$, Rel Error = 10^{-8} and Abs Error = 10^{-7}, CPU run time = 38 mins	28
4.5	Plot showing various boundary conditions simulated and time lapse plot of estrogen not docking into receptor.	30

4.6 The plot of Net Force Vs Time on Body A, with and without Scaling showing the scaled forces retaining the dynamics of the system. 31

4.7 Plot showing q_1 Vs Time for Body A *with and without* Brownian motion for scaled and unscaled system. $q_1 = 30$, $q_2 = 20$, Rel Error = 10^{-8} and Abs Error = 10^{-7} 32

A.1 The figure shows mass centers of the bodies used in this model 36

A.2 The locations of coarse grained Estrogen 37

B.1 Inertia calculation 40

D.1 Brownian Motion acting on Estrogen 45

LIST OF TABLES

Table		Page
3.1	Charge Values in Coloumbs	21
3.2	Bond Distances and repulsive constants	22
4.1	Various boundary conditions simulated.	29
A.1	Masses used in model	36
A.2	Locations of the bodies and points used in the model.	38
B.1	Covalent Radii of individual atoms.	41
C.1	Rotational and Translational Drag coefficients calculated.	43

CHAPTER 1

Introduction

It is predicted that this year, more than 1 million Americans and more than 10 million people worldwide will be diagnosed with cancer. Only 5 to 10 percent of all cancer cases can be attributed to genetic defects, whereas the remaining 90 to 95 percent have their roots in the environment [1]. It has been suggested that some chemical compounds have a similar structure and properties as natural hormones produced by the human body [2, 3]. Hence they can trigger the release of growth hormones that lead to unnatural tissue growth, and ultimately the tumors indicative of cancer.

There is a need for identifying these chemical compounds for their endocrine disrupting nature. The U.S. Food and Drug Administration (FDA) mandates toxicity testing using Binding Assay method (an experimental method) for all new chemicals that have significant human and environmental exposure [4]. However, the binding assay is slow, costly, and labor intensive [5].

The current theoretical methods employed are molecular dynamic simulations (MDS), which are computationally intensive and therefore costly and slow. The proposed approach is theoretical and uses new tools developed for coarse graining and multi scale modeling to *drastically* decrease simulation run time, yielding a fast, inexpensive, efficient solution for screening carcinogens.

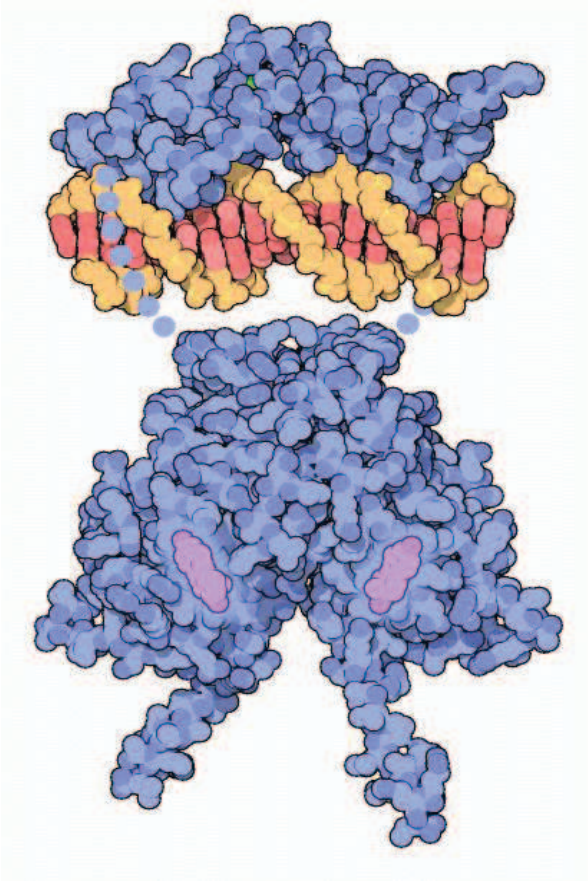

(a) Estrogen Receptor Dimer interacting with the DNA

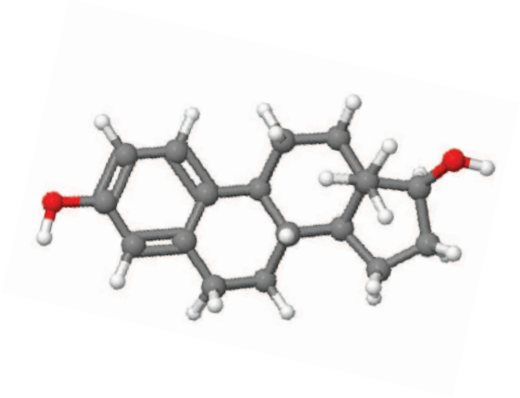

(b) 17β-Estradiol

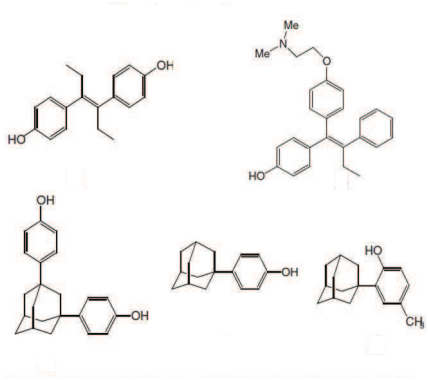

(c) XenoEstrogens [6]

Figure 1.1: Estrogen Receptor, 17β-Estradiol and Xenoestrogens

We will use breast cancer as the example for this study. The natural estrogen, 17β-Estradiol (See, Fig.1.1b) docks into the receptor, producing a conformational change and forming a dimer. The dimer interacts with the DNA (See, Fig.1.1a), causing growth protein production and eventually tissue growth.

Although there are hundreds of chemical compounds that can mimic certain properties of natural estrogen, referred to as *XenoEstrogens* (See, Fig.1.1c), they all do not result in breast cancer. Although there are several steps in this process, the hypothesis considered here is that the physical shape or configuration of the

XenoEstrogen, along with the intensity of its chemical charge, affects how it binds to the receptor [7].

The goal of this thesis is to provide a first generation model of estrogen docking into its receptor, thereby understanding the mechanism of docking and providing a platform to develop the screening technique. The goal of this screening technique is to provide a low cost and fast method to screen the environmental chemicals for their ability to dock into the receptor. Considering the advantages of this new theoretical approach, the cost of preliminary screening could be greatly reduced, providing a valuable tool to the FDA.

The author's contribution to this work includes:

1. Coarse graining and modeling the Estrogen molecule.
2. Modeling the hydrogen bonding, drag forces, inertia and Brownian motion.
3. Providing a first generation model to develop a theoretical based screening methodology.
4. Classifying and addressing the nature of the multi scale modeling of small molecules.

CHAPTER 2

Background

There are three major naturally occurring estrogens: Estrone (E1), Estradiol (E2) and Estriol (E3), numbered after the number of -OH groups in their molecular structure. Estradiol (E2 or 17β-Estradiol) is considered to be the predominant estrogen in terms of the estrogenic activity and hence it is used in this thesis. In the rest of this manuscript, for convenience, the 17β-Estradiol will be referred to Estrogen.

A ligand is a chemical that "docks" or "binds" to the receptor. A ligand binding domain (LBD) is the "site" in the receptor at which the ligand "binds" the receptor.

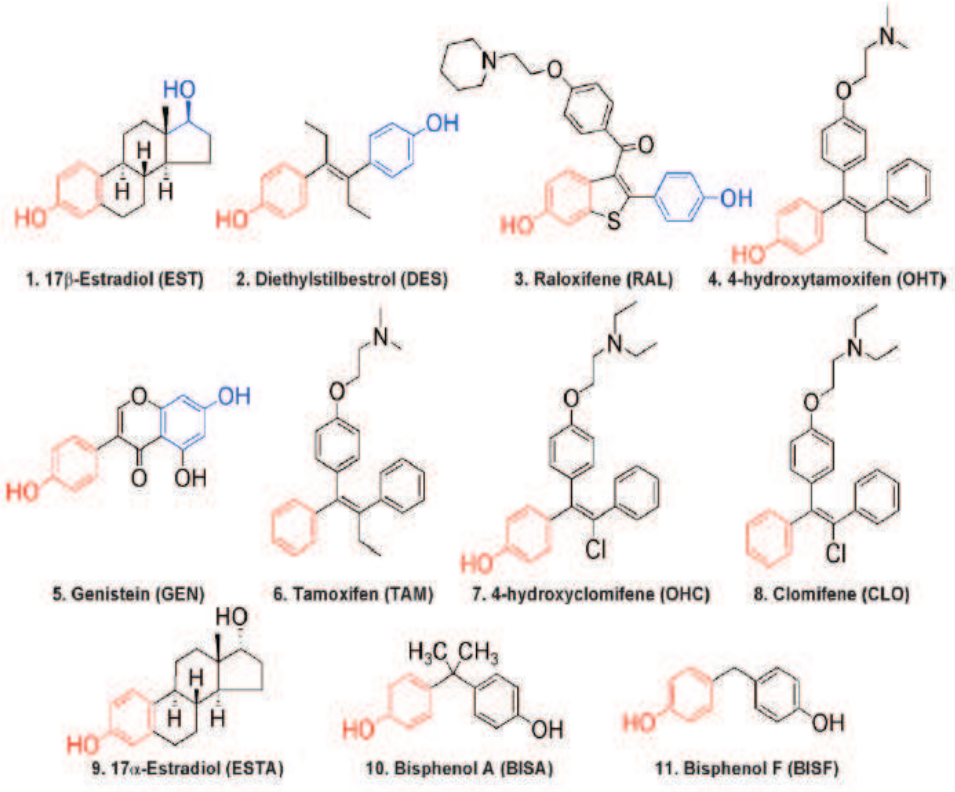

Figure 2.1: Xenoestrogen Examples [7]

There are a wide variety of chemical structures that can potentially bind with the estrogen receptor (ER) and trigger estrogenic activity in humans, referred to as *XenoEstrogens* [6]. Fig.2.1 shows some common XenoEstrogens identified experimentally [5, 7].

This section is a brief overview of the experimental and theoretical studies performed on the various estrogens and its receptor.

Experimental Studies:

The *in vivo* (In the body) experimental methods are required to identify adverse effects produced by the environmental chemicals, but they are costly and time consuming. Hence, the *in vitro* (Out of body, in lab) assays are currently used for screening of endocrine disrupting chemicals [8]. In this section, the *in vitro* experimental methods are referred to as experimental methods for convenience.

One of the widely used methods is the ligand-binding assay (LBA) experiments. They utilize a competitive-binding assay to determine the receptor's affinity to environmental chemicals [5, 9] and are currently used by Food and Drug Administration for screening [10]. The structure-activity relationship studies were performed on a diverse group of environmental chemicals based on the competitive binding assay experiments and they identified five distinguishing criteria in a chemical that were found to be essential for estrogenic activity:

1. H-bonding ability of the phenolic ring mimicking the 3-OH.
2. H-bond donor mimicking the 17β-OH and O-O distance between 3- and 17β-OH.
3. Steric hydrophobic centers mimicking steric 7α- and 11β-substituents.
4. Hydrophobicity of the molecule.
5. A ring structure [11].

These factors were being used as the first step in screening environmental chemicals.

The Fluorescent Polarization (FP) method uses a ligand tagged with radio active fluorescence and hence can detect chemicals with weak estrogenic activity compared to the LBA experiments [8, 12, 13, 14]. On the other hand, there were studies to assess the potency of the mixture of environmental estrogens to trigger the ER [15, 16].

However, experimental screening is based on the symptoms instead of the nature of the chemical. Hence, the chemical's concentration is an important factor that determines the outcome [5]. The experimental screening also takes up time, involves costly setup and is prone to human error and hence the theoretical methods are preferred for screening.

Theoretical Studies:

The theoretical methods were used to study the structure of docked estrogen and also the charge distribution on naturally occurring estrogens.

The X-Ray diffraction studies were performed to study the the LBD of the Estrogen Receptor [17, 18, 19, 20]; these studies reveal important details on the factors that trigger the bonding of estrogen into its receptor. The crystallographic structure between the LBDs of estrogen and progesterone are compared identifying the common factors between the two naturally occuring chemicals [21, 22].

Molecular Dynamics is the science of simulating the motions of a system of particles [23]; these simulations are used to study the conformational dynamics of the ER [24]. The Molecular Dynamic Simulations (MDS) performed on the estrogen bounded ER highlight the importance of the charge transfer between the ER and its ligands in determining the conformational change in the receptor and hence the potency of the estrogen [7]. These MDS studies identify that the charge and structure

of the ligand are the key factors for docking. Hence, charge density studies were performed using various models to study the charge distribution on various chemicals.

Ab initio quantum chemistry methods are computational chemistry methods based on quantum chemistry and these studies are used to theoretically calculate the Relative Binding Affinity of the environmental chemicals, which determine the potency of the natural chemical [23]. Charge density studies were performed to understand the charge distribution on the estrone (E1) [25, 26] and estradiol (E2) [25, 27]. Hansen-Coppens multi-pole models were used to study the charge distribution on the 17α-Estradiol, an isomer of 17β-Estradiol [28, 25]. The Fragment Molecular Orbital (FMO) methods use quantum-chemical wave functions to model the atomic behavior. These were used in drug design to treat breast cancer [29, 30]. CHARMM Analysis (Chemistry at HARvard Molecular Mechanics) is a widely popular molecular simulation method that could be used to perform MDS on the system [31]. The custom coarse graining option in the CHARMM analysis is a tool that could be potentially be used for screening, however, the CHARMM analysis is too broad and costly to provide a tool tailored for screening. Computer-based quantitative structure-activity relationship models (QSAR) are regression models used in the chemical and biological sciences. These models relate a set of "predictor" variables (atom by atom position on the xenoestrogens), to the potency of the response variable (the ability of the xenoestrogen to trigger the Estrogen receptor). These models were developed to be used as a theoretical screening technique for carcinogens [32].

The lengthy run time for MDS results from modeling each atom in a molecule and all of the interactions between them. These interactions include high frequency vibrations and oscillations between the atoms that require a very small time step to capture.

The author could not identify the dynamics of docking being studied in the literature. Hence, this work is a first generation approach to model and understand the docking of estrogen into the receptor.

CHAPTER 3

Method Implemented

3.1 Rigid multibody model

Coarse-graining is a technique to represent a system by a reduced (in comparison with an all-atom description) number of degrees of freedom. Hence, a set of rigid bodies are used in a coarse grained system to reduce the degrees of freedom compared to the all atom representation, thereby yielding low simulation time. In rigid body based models, the inertia terms related to the mass distribution, the coriolis, and the centripetal terms are retained in order to remain true to the original molecular dynamic model [33]. Here, a coarse grained 2D mechanical model is used, having the features shown in Fig.3.1b, which is not drawn to scale. This model represents the Ligand Binding Domain (LBD) of the Estrogen Receptor (ER), as revealed from the X-Ray crystal diffraction studies as shown in Fig.3.1a [17].

The objectives of this paper can be sufficiently met with the following assumptions:

1. Only the LBD of the ER is considered and Hydrogens of the ER have comformational change (Bodies E and F in Fig.3.1b).
2. In the estrogen molecule, the Hydrogens (Bodies B and C in Fig.3.1b) undergo comformational change while the rest of the Estrogen is modeled as a rigid body (Body A in Fig.3.1b).
3. The effect of interatomic vibrations are ignored.

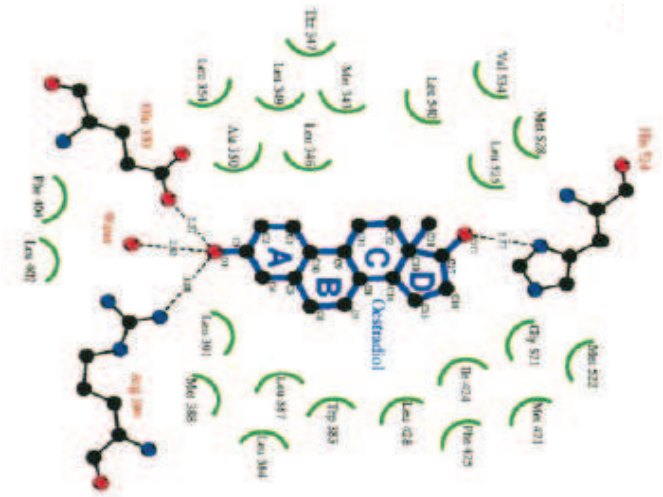

(a) The docked estrogen forming four hydrogen bonds with the receptor. The dotted lines indicate the hydrogen bonds and the green lines indicate the estrogen receptor "locking" the estrogen in place. Notice that the Hydrogens are not explicitly shown in the model.

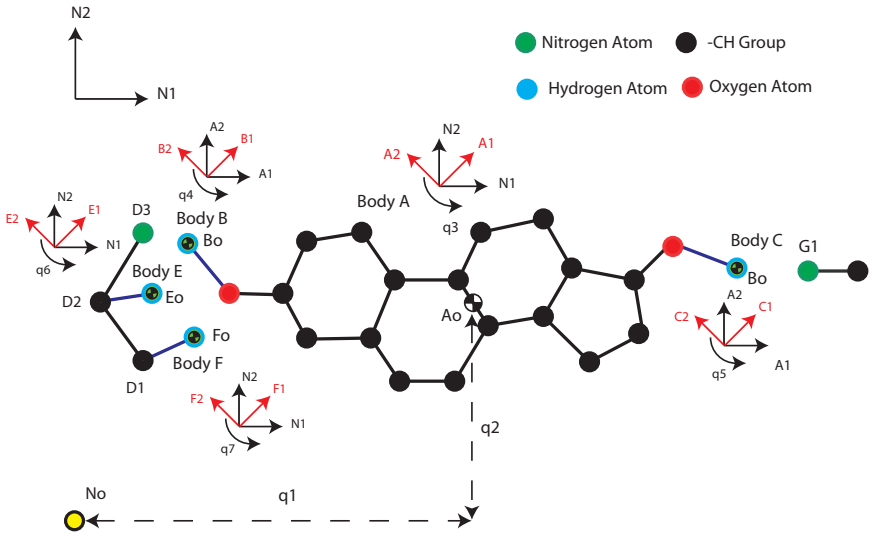

(b) Schematic representation of Estrogen showing different rigid bodies and points used in the model.

Figure 3.1: Figure showing the estrogen docked in the receptor as revelaed from the diffraction studies and the coarse grained model used in this work.

The mechanical model is comprised of ball and socket connected rigid bodies as shown in Fig.3.1b. The rest of the atoms on the Estrogen molecule are modeled as massless points, represented by the black dots. The mass centers of each body are represented by the small half-filled circles. For detailed description about the location of individual points, see Appendix A. The bodies E, F and points D1, D2, D3 and G1 represent the ER and any comformational changes in the receptor other than that of hydrogens are neglected.

The vectors *N1* and *N2* in Fig.3.1b define the *inertial reference frame*. All other reference frames are attached to the different bodies. Fig.3.1b, body A has three degrees of freedom denoted by q_1, q_2 and q_3. The angular rotation of body A about the *N3 (= N1 × N2)* direction is represented by q_3. The angular rotation of bodies B and C about the $A3$ axes is represented by q_4 and q_5 respectively. Bodies E and F have angular rotations of q_6 and q_7 about the $N3$ axis, hinged at D1 and D2 respectively. The multibody mechanical model has the form

$$A(\mathbf{q})\ \ddot{\mathbf{q}}\ +\ \mathbf{b}(\dot{\mathbf{q}},\mathbf{q})\ =\ \underbrace{\sum \mathbf{\Gamma}(\dot{\mathbf{q}},\mathbf{q})}_{active forces} \tag{3.1}$$

where $\mathbf{q} = [\mathrm{q}_1 \cdots \mathrm{q}_7]^T$ contains the generalized coordinates in Fig. 3.1b, and $\dot{\mathbf{q}}$ and $\ddot{\mathbf{q}}$ are its time derivatives of generalized speeds and accelerations. The term $A(q) \in \mathbb{R}^{7\times 7}$ is the mass matrix. The forces on the left of Eq.3.1 are referred to as *generalized inertia forces* since they depend on mass.

The forces on the right of Eq.3.1 are referred to as *generalized active forces* defined as

$$\sum \mathbf{\Gamma} = \mathbf{\Gamma}_{Friction} + \mathbf{\Gamma}_{Charge} + \mathbf{\Gamma}_{Brown} \tag{3.2}$$

$$\mathbf{\Gamma}_{Friction}\ =\ -\beta\ D(\mathbf{q})\ \dot{\mathbf{q}} \tag{3.3}$$

where β is the viscous damping coefficient and $D \in \mathbb{R}^{7\times7}$ is a function of $\mathbf{q}$, which transforms friction forces and moments applied at the mass center of each body into generalized active forces. The vectors $\mathbf{\Gamma}_{Charge}$, and $\mathbf{\Gamma}_{Brown}$ contain forces related to Charges and Brownian motion. These forces are discussed in detail in the following sections.

The unit of mass, the *Zeptogram* (zg), is chosen so that the mass values are on the order 10^0, and the length and time units, the *Angstrom* ($\mathring{A}$) and *Nanoseconds* (ns), are chosen for similar reasons. These masses and inertias are contained in the mass matrix $A(\mathbf{q})$ in Eq.3.1, which is symmetric, positive definite and non-diagonal.

3.2 Multi Scale Analysis

The Multiscale features of physical and biological phenomena occur because of disproportionality at two different scales:

1. Different structural length scales of those phenomena and
2. The External interactions of the system with environment [48].

In this model, although there is a Protien interacting with a Molecule, which involves two different length scales, only the Ligand Binding Domain of the Protien is considered and hence, this system effectively has only one length scale.

For the interaction with the environment, one of the criteria used to classify the system for its multi scale nature is the ratio of mass over the drag coefficient ($\frac{m}{\beta}$). If, this ratio ($\frac{m}{\beta}$) is high, then the interaction could probably be a multi scale problem. The $\frac{m}{\beta}$ value for this system is $O(10^{-5})$ which does not clearly define the multiscale nature of this system. One of the characterstic of a multi scale problem is the long CPU run time and for a $20ns$ simulation, the CPU run time was 38 mins which is large. Hence, this system is classified as a multi scale problem and the following procedure indicates one of the ways to address the multi scale nature of the system.

Applying the Newton's second law to the system yields a different form of Eq.3.1:

$$m_{tot}\ \ddot{\mathbf{x}} = \underbrace{\mathbf{F} - \beta\dot{\mathbf{x}}}_{\text{active forces}} \tag{3.4}$$

Dividing both sides of Eq.3.4 by viscous coefficient, β, yields,

$$\mathbf{0} \ = \ \frac{m_{tot}}{\beta}\ \ddot{\mathbf{x}} = \frac{\mathbf{F}}{\beta} \ - \ \dot{\mathbf{x}} \tag{3.5}$$

where $\ddot{\mathbf{x}}$ and $\dot{\mathbf{x}}$ are vectors of acceleration and velocity, $m_{tot} = 0.45\ zg = 0.45 \times 10^{-23} gms$ is the total mass of Estrogen, $\beta \approx 10^4 zg/ns$ (See Eq.3.25) is the coefficient of viscous friction, and F is a vector of other external forces (See Eq.3.2).

The disproportionate size of the mass and viscous friction produce the small coefficient in Eq.3.5, yielding large accelerations that are difficult to numerically integrate. Reducing the time unit/scale to attoseconds, $1as = 10^{-18}s$, yields a coefficient of $O(10^0)$ that is easier to integrate; all terms in Eq.3.5 have units of $\mathring{A}/ns$ so changing the time unit does not fix disproportionality. This disproportionality can be solved by omitting the small term, solving for the velocity as $\dot{x} = F/\beta$, and integrating to find $x(t)$ [35, 36]. This is called the *massless, first order model* which forms the basis for the well-known Langevin [37, 38, 39] and Fokker-Planck equations [40, 41].

Alternately, techniques from the *method of multiple scales* (MMS) can be used to eliminate only the large forces that create large accelerations. The MMS allows an investigation of the model's behavior at different time scales. This process begins by determining a characteristically small number, $\epsilon = 2.2 \times 10^{-5}$ for a nanosecond time scale, $(1ns)\epsilon = m_{tot}/\beta$ from the model in Eq.3.5.

$$\mathbf{0} \;=\; \epsilon(1ns)\ddot{\mathbf{x}} \;-\; \frac{\mathbf{F}}{\beta} \;+\; \dot{\mathbf{x}} \tag{3.6}$$

The small parameter ϵ is used to decompose time into different scales, $T_i = \epsilon^i t$, yielding:

$$\dot{\mathbf{x}} = \frac{d\mathbf{x}}{dt} \;=\; \epsilon^0 \frac{\partial \mathbf{x}}{\partial T_0} \;+\; \epsilon^1 \frac{\partial \mathbf{x}}{\partial T_1} \;+\; \epsilon^2 \frac{\partial \mathbf{x}}{\partial T_2} \;+\; \cdots \tag{3.7}$$

$$\ddot{\mathbf{x}} \;=\; \frac{d^2\mathbf{x}}{dt^2} \;=\; \sum_{i=0}^{\infty}\sum_{j=0}^{\infty} \epsilon^i \epsilon^j \frac{\partial^2 \mathbf{x}}{\partial T_i \partial T_j} \tag{3.8}$$

Substituting Eq.3.7 and Eq.3.8 into Eq.3.5, and arranging in order of increasing power of ϵ yields

$$\mathbf{0} = \epsilon^0 \left(-\frac{\mathbf{F}}{\beta} + \frac{\partial \mathbf{x}}{\partial T_0} \right) + \epsilon^1 \left((1ns)\frac{\partial^2 \mathbf{x}}{\partial T_0^2} + \frac{\partial \mathbf{x}}{\partial T_1} \right) + \cdots \tag{3.9}$$

The difference between $\epsilon^0 = 1$ and $\epsilon^1 = 2.2 \times 10^{-5}$ is large, so it is likely that the *active forces* in Eq.3.4 must cancel to some extent for the sum in Eq.3.9 to equal zero.

This is acomplished by decomposing the ϵ_0 term, into large and small parts using scaling factors a_1 and a_2,

$$-\frac{\mathbf{F}}{\beta}+\frac{\partial \mathbf{x}}{\partial T_0} \;=\; (a_1 \;+\; a_2)\left(-\frac{\mathbf{F}}{\beta}+\frac{\partial \mathbf{x}}{\partial T_0}\right) \tag{3.10}$$

where $a_1 + a_2 = 1$ and $a_1 \gg a_2$. Herein, it is assumed that the large active forces, scaled by a_1, cancel.

$$\mathbf{0} = a_1\left(-\frac{\mathbf{F}}{\beta}+\frac{\partial \mathbf{x}}{\partial T_0}\right) \tag{3.11}$$

This implies that the small active forces do not cancel,

$$\mathbf{0} \neq a_2\left(-\frac{\mathbf{F}}{\beta}+\frac{\partial \mathbf{x}}{\partial T_0}\right) \tag{3.12}$$

but instead drive the estrogen. The scaling in Eq.3.12 preserves the relative magnitudes between the constituent forces and brings them into proportion with the mass. Eq.3.6 is rewritten using scaling factors a_1 and a_2,

$$\epsilon(1ns)\ddot{\mathbf{x}} \;+\; (a_1 + a_2)\left(-\frac{\mathbf{F}}{\beta}+\dot{\mathbf{x}}\right) = \mathbf{0} \tag{3.13}$$

It is desired to remove the canceled forces from the original model. This can be acomplished by substituting Eq.3.11 into Eq.3.13, and assuming $\frac{\partial \mathbf{x}}{\partial t} = \frac{d\mathbf{x}}{dt}$.

$$\epsilon(1ms)\ddot{\mathbf{x}} \;+\; a_2\left(-\frac{\mathbf{F}}{\beta}+\dot{\mathbf{x}}\right) = \mathbf{0} \tag{3.14}$$

Multiplying Eq.3.14 by β yields a second order model,

$$m_{tot}\;\ddot{\mathbf{x}} \;=\; a_2\;\mathbf{F} \;-\; a_2\;\beta\;\dot{\mathbf{x}} \tag{3.15}$$

where a_2 is found by matching the speed or other characteristics of the predicted and observed motions. Since all of the terms in Eq.3.15 are in proportion, it can be numerically integrated *drastically* reducing the CPU run time.

3.3 Mass and Inertia Calculation

The mass of the system is calculated based on the individual atomic masses in the molecule. Body A contains, *18 - Carbon, 22 - Hydrogen and 2 - Oxygen* atoms and hence the atomic weight is $270.38 gms/mol$. The atomic weight is divided with Avagadro's number ($N_A = 6.022 \times 10^{23} mol^{-1}$), the number of molecules in one mole of a given substance, through which we get the mass of the body A: $44.23 zg$. The rest of the masses are calculated in similar manner (refer Appendix A).

For the simplicity, the following assumptions are made in calculating inertia:

1. Each atom is assumed to be a solid sphere.
2. The radius of each solid sphere is assumed to be the atom's *covalent radius*.

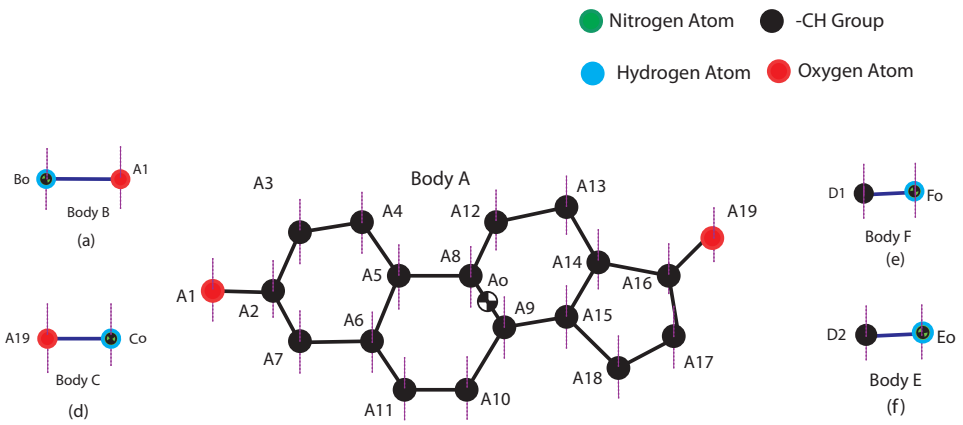

Figure 3.2: Figure shows the axis used to calculate the inertias for bodies

The inertias are calculated about the N_3 axis. Fig.3.2 shows the axis used for calculating the inertia of the bodies. The inertia of individual atoms are calculated about their mass center and are translated to the mass center of body A using *Parallel axis theorem*. For detailed description of the inertias refer to Appendix B.

3.4 Viscous Forces

The following assumptions are made for simplicity in calculating the drag force on this system:

1. The fluid is assumed to be Newtonian fluid with uniform viscosity at 20^oC.
2. Each atom is assumed to be a solid sphere and the *covalent radius* of atoms is used for the radius of sphere.

For calculating the viscous forces, the system falls in the transition region between the statistical and continuum mechanics formulation of fluid dynamics. A dimensionless Knudsen number (K_n) can be used to classify which formulation could be used.

Knudsen number is defined as the ratio of the molecular mean free path length of fluid (λ) to a representative physical length (L).

$$K_n = \frac{\lambda}{L} \tag{3.16}$$

If the Knudsen number is near or greater than one, the mean free path of a molecule is comparable to a length scale of the problem, and the continuum assumption of fluid mechanics is no longer a good approximation.

The λ_{water} is 2.5 $\mathring{A}$ and length scale of this problem is taken to be length of body A, $11.38\mathring{A}$ which implies that the K_n is 0.22. Since $K_n < 1$, an adjustment for Stokes law can be used to calculate viscous forces.

The derivation of Stokes law assumes no-slip condition which becomes inaccurate at high Knudsen numbers, *i.e.* for small particles. The Cunningham slip correction factor (C_c) allows predicting the drag force with Knudsen number between the continuum regime and free molecular flow as shown in Eq.3.17 [42, 43].

$$C_c = 1 + \frac{2\lambda}{L}[1.257 + 0.4e^{\frac{-1.1L}{2\lambda}}] \tag{3.17}$$

The calculated correction factor (C_c) is 1.614. The drag force is calculated based on the corrected Drag coefficient (β_{cc}).

$$\beta_{cc} = \frac{\beta}{C_c} \tag{3.18}$$

The linear drag coefficient (β) and rotational drag coefficients (β_w) for a sphere is given by

$$\beta = 6\pi\mu r \tag{3.19}$$

$$\beta_w = 8\pi\mu r^3 \tag{3.20}$$

where μ - Viscosity of medium and r - radius of the sphere. The viscous force and torque can be calculated from modified Stroke's law:

$$\mathbf{F_{drag}} = -\beta_{cc} \times^N V^A \tag{3.21}$$

$$\mathbf{T_{drag}} = -(\beta_w)_{cc} \times^N \omega^A \tag{3.22}$$

The viscous forces calculated from Eq.'s 3.21, 3.22 are applied on the system as shown in Fig.3.3, where the arrows indicate the drag forces and torques applied.

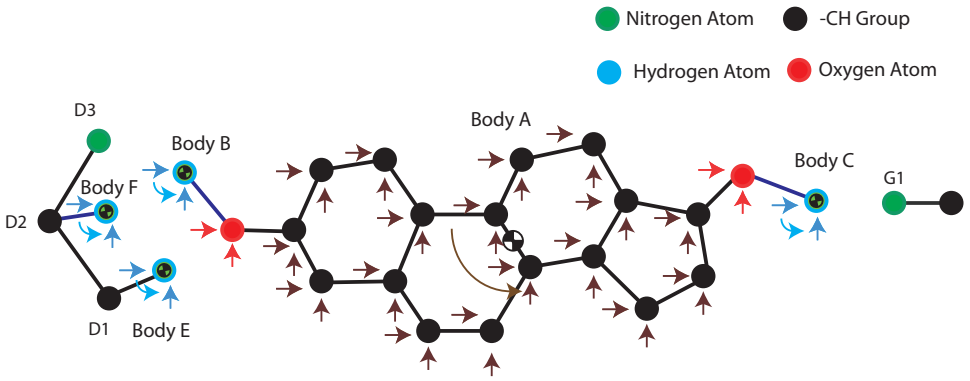

Figure 3.3: Drag forces on Estrogen

Note the difference in colors of the arrows used to imply forces in Fig.3.3, to indicate the difference in drag coefficients for different atoms. Refer Appendix C for detailed viscous force and torque calculations.

Considering the complicated shape of body A, an approximate value of β is calculated using Eq.3.25.

$$\beta_x = \frac{\sum Fx_{drag}}{{}^{N_1}V^A} \tag{3.23}$$

$$\beta_y = \frac{\sum Fy_{drag}}{{}^{N_2}V^A} \tag{3.24}$$

$$\beta = \sqrt{{\beta_x}^2 + {\beta_y}^2} \tag{3.25}$$

where Fx_{Drag}, Fy_{Drag} are drag forces in N_1 and N_2 direction modeled on each point on body A, as shown in Fig.3.3. ${}^{N_1}V^A$ and ${}^{N_2}V^A$ are the velocities of A along N_1 and N_2 direction. The β calculated from Eq.3.25 is $O(10^4)$.

3.5 Charge Forces

The docked 17β-Estradiol forms four hydrogen bonds with the ER as shown in Fig.3.4a. The following assumptions are made in this model:

1. Since, the potential of the Hydrogen bonding is complex to model [44], for simplicity, the coloumb potential is used.
2. Modified Hard Sphere repulsion is used to model the repulsive forces that exist when the atoms get closer than their Vanderwalls radii.

The magenta lines in the Fig.3.4a indicate the hydrogen bonds formed between estrogen and its receptor.

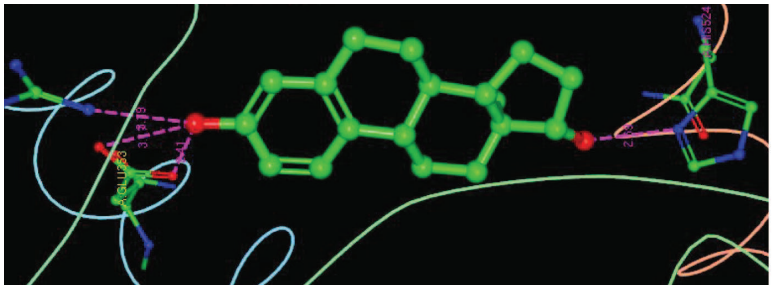

(a) Magenta lines indicate the Hydrogen bonds between the estrogen and its receptor, notice that the hydrogen atoms are not shown, www.rscb.org

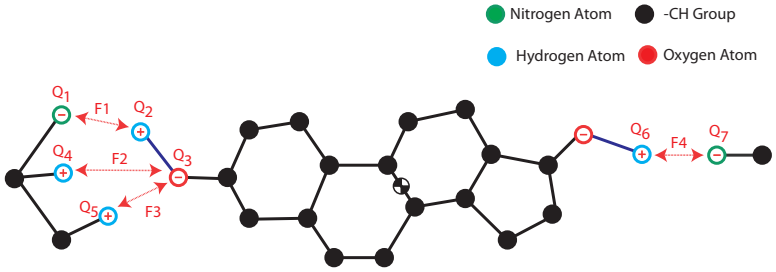

(b) F1, F2, F3 and F4 represent the force due to hydrogen bonds and are modeled using Eq.3.29. The values of charges $Q_1, \ldots, Q_7$ are given in Tab.3.1

Figure 3.4: Figure showing the forces due to hydrogen bonds.

Attractive Potential:

The Interaction potential of the Columb charge or Columb potential, w_a is a function of distance between the charges, r and is given by the relation, Eq.3.26 [44].

$$w_a(r) = \frac{Q_1 Q_2}{4\pi\epsilon r} \tag{3.26}$$

where $w_a(r)$ - Columb Potential, Q_1, Q_2 - Columb Charges, ϵ - Permittivity of the medium ($\epsilon = \epsilon_o \epsilon_r$, where ϵ_o - Permittivity of Vaccum and ϵ_r - Relative Permittivity of medium) and r - Distance between charges.

Repulsive Potential:

The nature of the attractive force is to attract the charges till the distance between them, r tends to zero. However, the atoms are like hard spheres with a

Table 3.1: Charge Values in Coloumbs

Charge	Q_1	Q_2	Q_3	Q_4	Q_5	Q_6	Q_7
Value	-1.593	0.62	-1.41	2.203	0.60	1.363	-0.632

radius as *Vander walls* radius. When the spheres collide with each other, the distance between the mass centers of the spheres is equal to the sum of their radii and not zero. At the point of collision, there exists a repulsive force between the atoms. This repulsive force is called har sphere repulsion and can be numerically modeled using Eq.3.27 [44].

$$w_r(r) = \frac{B_1}{r^6} \tag{3.27}$$

where w_r - Repulsive Potential, B_1 - Constant and r - Distance between Charges. For large values of r, the value of w_r is very small and the distance, r at which w_r starts to increase is dependent on the constant $B1$ which is discussed below.

Total Interaction Potential:

The Interaction potential, w of a bond is the sum of the coloumb (Eq.3.26) and repulsive potential (Eq.3.27).

$$w(r) = w_a(r) + w_r(r) = \frac{1}{4\pi\epsilon}\left[\frac{Q_1Q_2}{r} + \frac{B}{r^6}\right] \tag{3.28}$$

The net force, $F(r)$ can be calculated by taking the derivative of interaction energy with respect to the distance as shown in Eq.3.29

$$F(r) = \frac{dw(r)}{dr} \tag{3.29}$$

The charge values $Q_1, \ldots, Q_7$ in Fig.3.4b are taken from the charge density studies [27] and from the *Ab initio* Quantum Mechanical studies [7]. The values used are shown in Table.3.1.

Using the Eq.3.29 and the values of charges from Table.3.1, the charge forces are modeled as shown in Fig.3.4b.

Table 3.2: Bond Distances and repulsive constants

Force	Bond Distance ($\mathring{A}$)	B
F1	2.37	12.3
F2	2.4	41.22
F3	2.82	57.12
F4	2.7	9.06

The bond distances used in this model are show in the Table.3.2 [27]. The constant B in the repulsive potential from Eq.3.28, can define the point at which the interaction potential for a bond is minimum, in other words, the forces between the atoms is zero at this point and hence, the system is in equilibrium. The value of the constant B is calculated by finding the local minimum of the total interaction potential in Eq.3.28, when r is equal to bond distance of the Hydrogen bond [27].

The Fig.3.5 gives a sample graph of interaction potential Vs distance. The point X shows the distance at which the potential value is minumum, the bond distance and the Force at that point is equal to zero. Notice the steep raise in the interaction potential as the distance r is less than the bond distance.

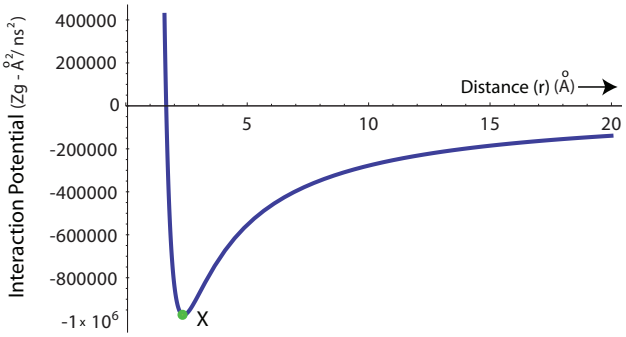

Figure 3.5: Graph of Interaction Potential vs Distance

3.6 Brownian Motion

This work, utilizes the already established method of modeling Brownian motion on Motor protiens in the lab [45].

Random forces and moments in the model, representing Brownian motion, are implemented as Gaussian white noise. The forces and torques due to brownian motion are modeled about each atom as shown in Fig.3.6 and are defined, for example, as

$$f_{Bo} = B_{o1}(t)N_1 + B_{o2}(t)N_2 \tag{3.30}$$

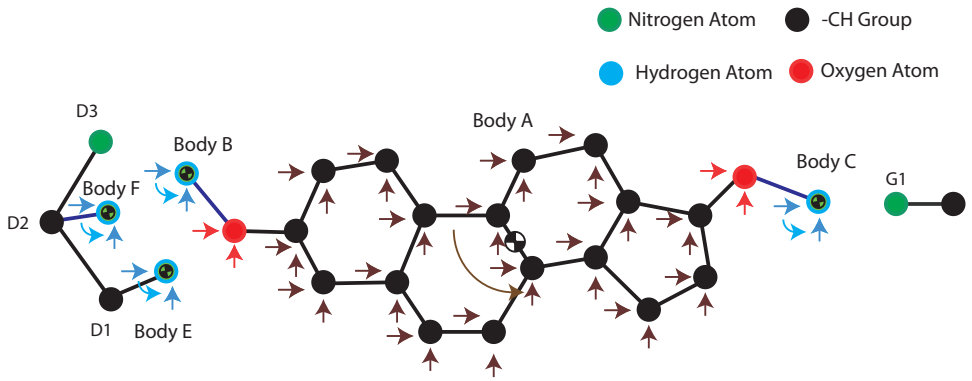

Figure 3.6: Brownian Motion acting on Estrogen

The $B_{o1}(t)$ represents forces produced by randomly fluctuating thermal noise on the body B. Each component of the random force and moment is treated independently as a normally distributed random variable. They have the following *expectations, E[.]*, or weighted average values,

$$E[B_{oi}(t)] = < B_{oi}(t) > = 0 = \mu \tag{3.31}$$

and are governed by a fluctuation - dissipation relaxation expressed as

$$E[B_{o1}(t_1)B_{o2}(t_2)] = 2\beta k_B T\delta(t_1 - t_2)\delta_{i,j} \tag{3.32}$$

where k_B and T are the Boltzmann constant and absolute temperature [46]. The relation in Eq.3.31 implies that there is no time dependency between the random

process over time; the random sequence of forces does not repeat regularly.

In addition, Eq.3.31, Eq.3.32 imply

$$E[B_{o1}^2(t)] = 2\beta k_B T = Var(C_{oi}(t)) = \sigma^2 \tag{3.33}$$

which is the variance of B_{oi}. Thus the B_{oi} can be generated using the Matlab function normrnd$(\mu, \sigma, \ldots)$ which generates random variables with a normal distribution. The collection of random forces comprise F_{Brown}. These randomly fluctuating discontinuous functions slow numerical integration so each random variable is held constant during a single integration step; the random variable is updated at the beginning of each step. Thus the value of each random variable is known before the integration step, and the decomposed value of the random force must equal it. This is accomplished by defining

$$F_{Brown} = (\beta_1 + 1) R_{nd} r_{nd} = (\beta_1 + 1) R_{nd} \begin{pmatrix} \bar{B}_{01} \\ \bar{B}_{02} \\ \bar{B}_{03} \\ \vdots \end{pmatrix} \tag{3.34}$$

where R_{nd} transforms the random forces into generalized active forces, and

$$B_{oi} = (\beta_1 + 1) \bar{B}_{oi} \tag{3.35}$$

and likewise for the other random forces. See Appendix D, for further details about modeling the Brownian motion.

CHAPTER 4

Results and Discussion

Without the Brownian Force:

The Fig.4.1 shows the screen shots of various steps in the estrogen docking into its receptor without brownian motion.

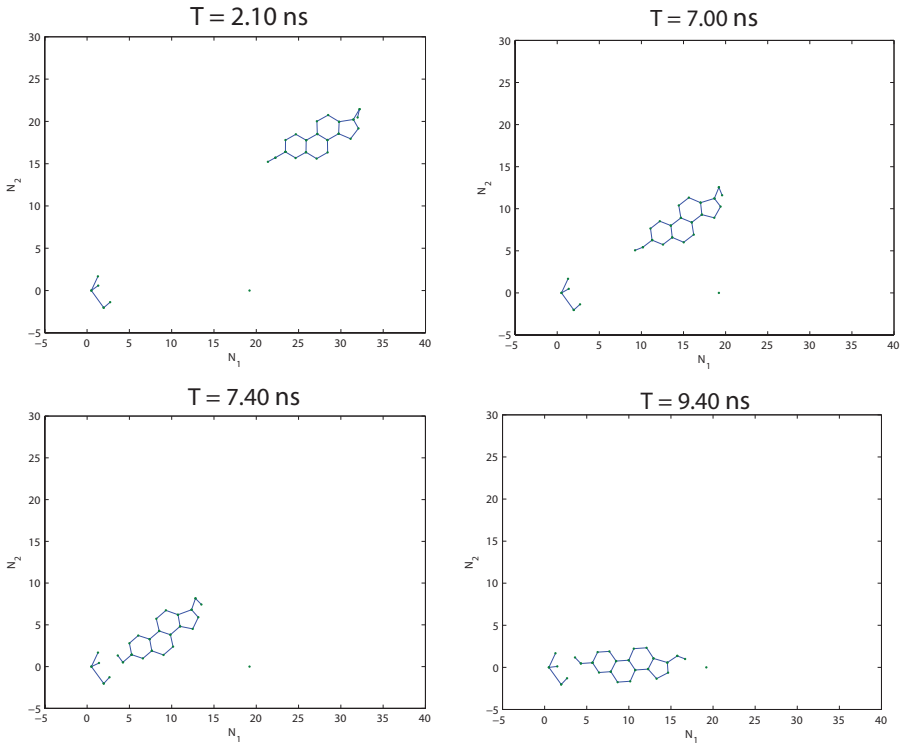

Figure 4.1: Simulation of Estrogen docking into its receptor, $q_1 = 30$, $q_2 = 20$, Rel Error $= 10^{-8}$ and Abs Error $= 10^{-7}$, CPU run time = 20 mins

In Fig.4.1, at *T = 2.10 ns*, the charge forces attract the estrogen towards receptor. Since the combined forces of the three charges (F1, F2, F3) at the front of

estrogen have greater force than the force (F4) at the other end (See, Fig.3.4b), the estrogen turns towards the before docking.

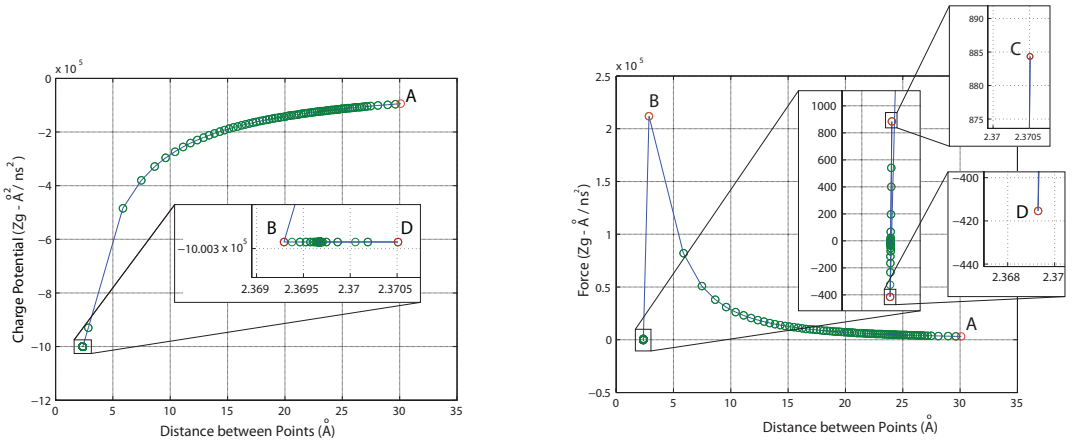

(a) Graph of Charge Potential Vs Distance

(b) Graph of Force Vs Distance

Figure 4.2: Graphs showing the Charge Potential and Force Vs Distance for one of the charges. The points A, B, C and D indicate various significant values during the docking.

At point A in Fig.4.2, the estrogen starts to move towards the receptor and the potential is at its maximum value and force at its minimum. Then as the estrogen approaches towards the receptor, the potential reduces and the force increases till it reaches the receptor at point B. The B, as shown in Fig.4.2b shows the force just before the docking, where the force is maximum. After the docking, the potential and the force remains constant. The points C and D in Fig.4.2b shows the maximum attraction and repulsion just before the final docking.

With the Brownian Force:

The brownian motion has a significant effect on the docking and causes a delays the docking process. See Fig.4.3a, the graph shows a plot of q_1 Vs Time (q_1 is the degree of freedom of the body A along N_1 direction).

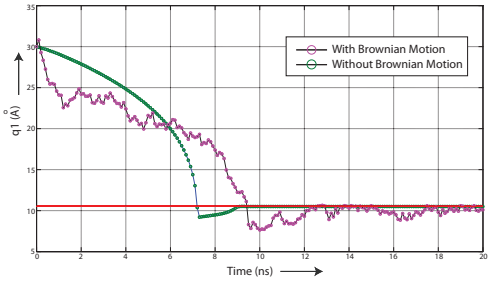

(a) Graph of q_1 Vs Time

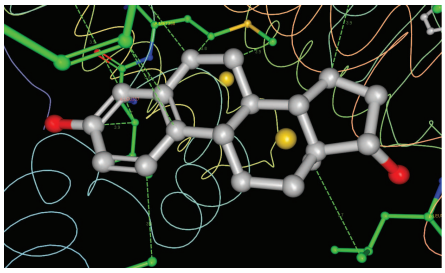

(b) Green lines represent hydrophobic bonds formed by docked estrogen, www.rscb.org

Figure 4.3: Figure shows the graph of q_1 Vs time with and without the brownian force and the hydrophobic bonds formed by docked Estrogen.

In Fig.4.3a, the horizontal red line shows the equilibrium position for q_1. The green dots represent the motion without the brownian motion and the molecule moves smoothly docking into the receptor at *9.1 ns*. The magenta dots represent the motion with the brownian motion, since the scale of brownian forces are in the same order as charge forces, they cause significant vibrations in the system. With brownian motion, the docking occurs at *10.7 ns*. After the docking, the force due to charges is not strong enough to cancel the force due to brownian motion and hence causes vibrations in the system which can be observed in Fig.4.3a.

After docking, the estrogen forms hydrophobic bonds with the neighboring receptor molecules as shown in Fig.4.3b causing conformational change in the receptor, locking the estrogen in place. Since, the estrogen receptor is not modeled in this work, the vibrations can be observed in the molecule even after the docking.

The Fig.4.4 shows the plot of force vs time for body A. The forces considered in this plot are just the magnitude of the total sum of forces acting on body. The red dots are the the brownian forces, green lines are the viscous forces and the black

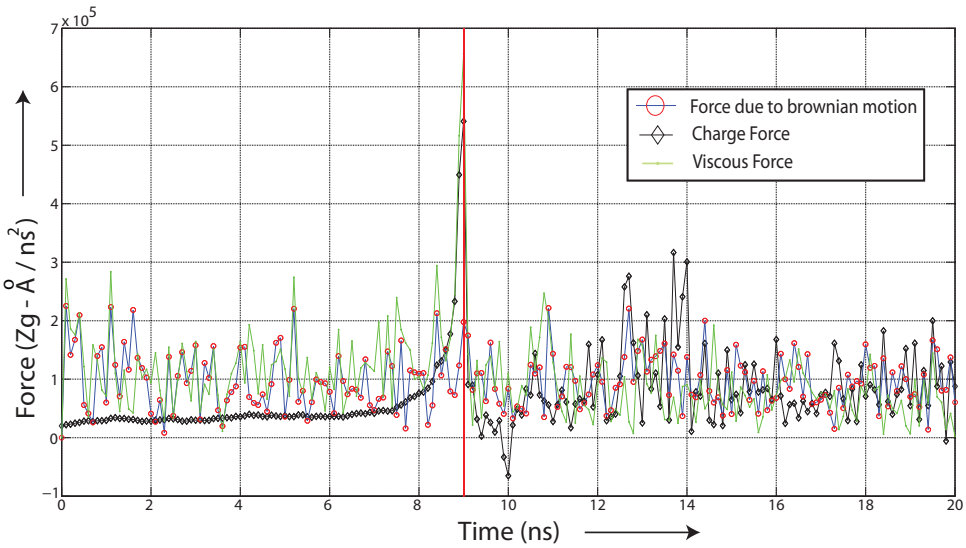

Figure 4.4: The plot of Force Vs Time, $q_1 = 30$, $q_2 = 20$, Rel Error $= 10^{-8}$ and Abs Error $= 10^{-7}$, CPU run time = 38 mins

diamonds are the sum of charge forces. While the brownian motion may appear to be the predominant force, the viscous forces dampen the brownian forces and the consistancy of the charge forces, binds the molecule in place. The red line indicates the time at which the docking occurs and the charge forces and the viscous forces reach the maximum value at that point.

Discussion:

The simulations were run for different boundary conditions with brownian motion, see Table.4.1 and the following observations are made:

1. The brownian motion decides the time the estrogen takes to dock and hence no specific analysis can be deducted from docking times.
2. The estrogen molecule appears to have failed to dock completely when placed below or behind the estrogen receptor as shown in Fig.4.5b, this could be because of the charge force (F4) is not strong enough to over come the brownian motion and complete the docking.

Table 4.1: Various boundary conditions simulated.

S.No.	q_1 ($\mathring{A}$)	q_2 ($\mathring{A}$)	q_3 (Deg)	Brownian Force	Time to dock (ns)	Complete Docking
1.	30	20	0	No (N)	9.1	Yes (Y)
2.	30	20	0	Y	10.7	Y
3.	30	20	180	Y	11.3	Y
4.	30	-20	0	Y	3.5	Y
5.	50	20	0	Y	32.3	Y
6.	-30	-20	0	Y	19.6	N
7.	-50	20	0	Y	49.6	N
8.	50	0	0	Y	19.3	Y
9.	-50	0	0	Y	40.5	N
10.	10	50	0	Y	45.3	Y
11.	10	-50	0	Y	15.2	N
12.	40	20	0	Y	14.2	Y
13.	60	20	0	Y	46.2	Y
14.	70	20	0	Y	73.5	Y
15.	80	20	0	Y	90.6	Y
16.	90	20	0	Y	123.2	Y
17.	100	20	0	Y	140.5	Y
18.	10	-60	0	Y	20.6	N

3. Based on the data, the region on the right of the red lines shown in Fig.4.5a appears to be the favourable region through which the estrogen could approach the receptor.
4. In the boundary conditions at which the estrogen fails to dock into the receptor, it could be assumed that the ER should have directed or guided the estrogen to complete its docking.

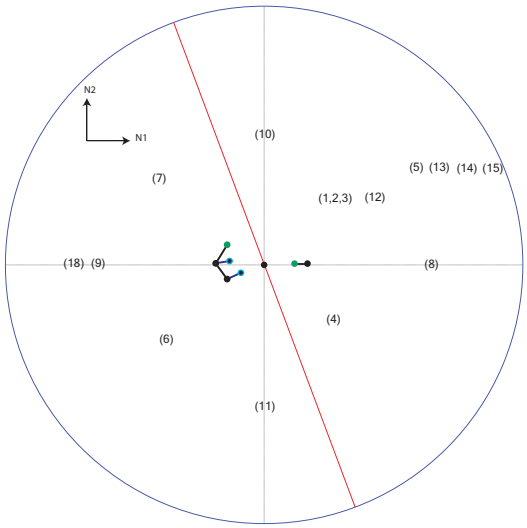

(a) Positions of various boundary conditions simulated, See Table.4.1

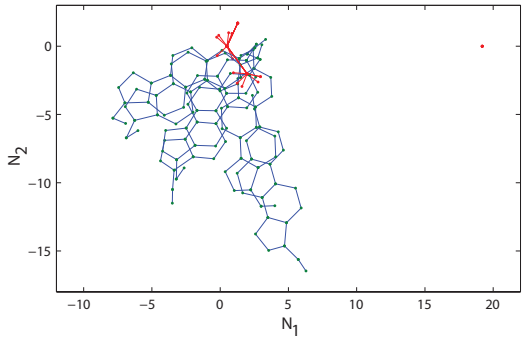

(b) Time lapse simulation of estrogen not docking into the receptor with brownian motion, Time to dock: *35 ns*, q_1 = 10, q_2 = -50, Rel Error = 10^{-8} and Abs Error = 10^{-7}, CPU run time = 62 mins

Figure 4.5: Plot showing various boundary conditions simulated and time lapse plot of estrogen not docking into receptor.

Multiscale issues:

A further analysis on the forces acting on the body A reveals that the forces do not cancel each other out as shown in Fig.4.6a. The forces are in $O(10^5)$, causing large accelerations, forcing the small time of integration in the order of attoseconds ($10^{-18} sec$). This small time step is causing large run times of *38 min* for a relatively small simulation time $20ns$. The Fig.4.6b shows the resultant forces on body A after the multi scale analysis with the scaling factor $a_2 = 3.2 \times 10^{-3}$ in Eq.3.15. The a_2 is determined by equating the positions of the body A without brownian motion as shown in Fig.4.7a.

It can be observed that the forces are in the same order as the mass of the system, thereby causing accelerations in the same order thereby achieving a *drastic* reduction in CPU run time upto 97%.

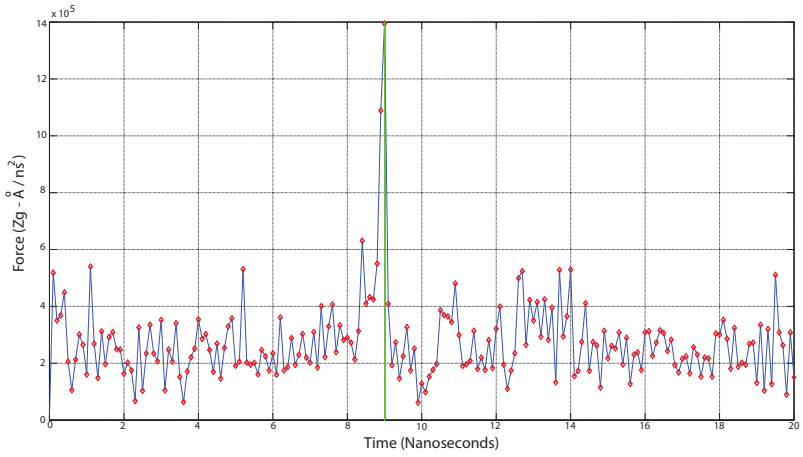

(a) Without Scaling

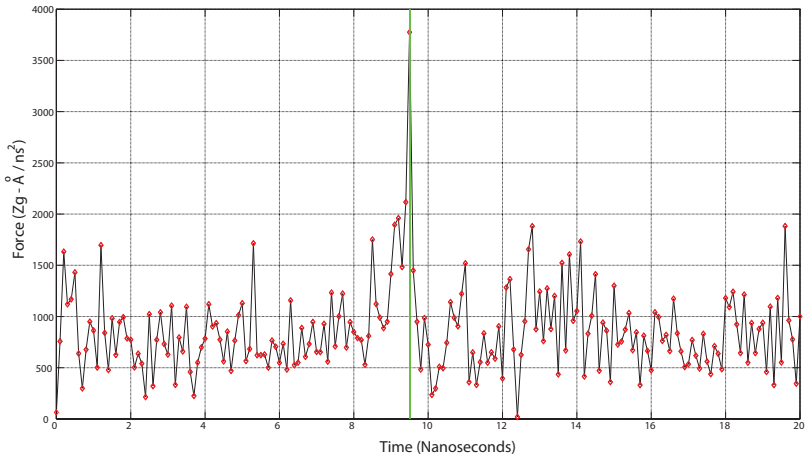

(b) With Scaling

Figure 4.6: The plot of Net Force Vs Time on Body A, with and without Scaling showing the scaled forces retaining the dynamics of the system.

In the Fig.4.7a and Fig.4.7b, it can be noted that the behaviour of the system is same with and without the scaling factor, which implies that the dynamics of the system does not get effected while reducing the CPU run time of the system. Hence, the multi scale analysis could be effectively used to reduce the CPU run time while retaining the dynamics of the system.

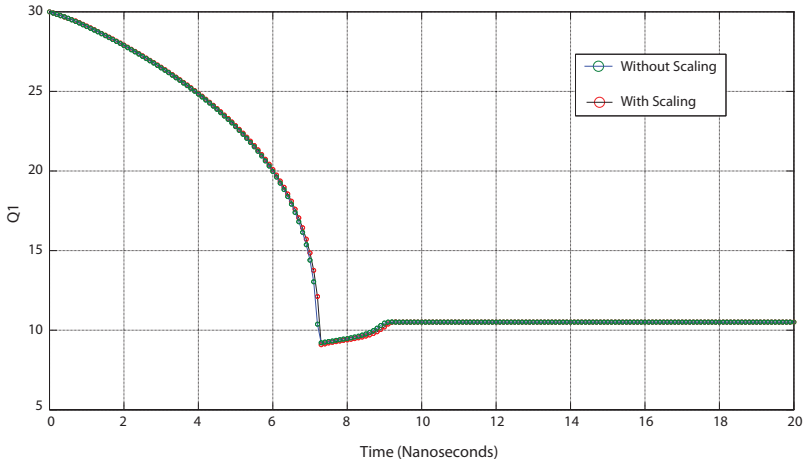

(a) Without brownian motion, CPU run time, without scaling = 26 mins, with scaling = 30 secs

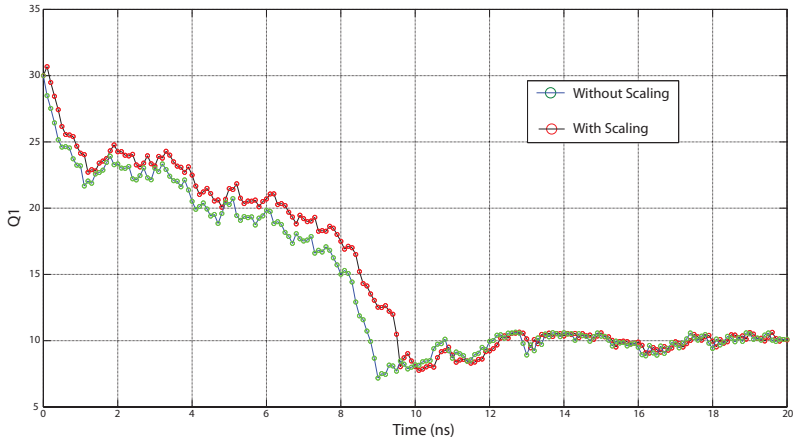

(b) With brownian motion, CPU run time, without scaling = 38 mins, with scaling = 45 secs

Figure 4.7: Plot showing q_1 Vs Time for Body A *with and without* Brownian motion for scaled and unscaled system. $q_1 = 30$, $q_2 = 20$, Rel Error = 10^{-8} and Abs Error = 10^{-7}

Future Scope:

There are many assumptions that put into this work to get the first generation model. Because of the time constraint, all the assumptions could not be validated. Following improvements needs to be made for this work:

1. Three Dimensional model of estrogen and the estrogen receptor needs to be modeled.
2. A more accurate modeling of hydrogen bonding could be used.
3. The viscous parameters used in this model can be validated with literature.
4. Since experimental validation of this work is difficult, a theoretical validation could help determine a degree of accuracy for this work.
5. Eventually, these simulations can be performed on the proven carcinogens to determine the degree of accuracy of this model as a theoretical screening technique.
6. Finally, a standard procedure can be developed to complete the theoretical approach to screen the environmental chemicals.

CHAPTER 5

Conclusion

A first generation model of estrogen docking into its receptor is presented. There is a need for a low cost, fast, theoretical approach to screen the environmental chemicals for their endocrine disrupting nature and this is the motivation for this work. The estrogen and Ligand Binding Domain of the Estrogen Receptor are coarse grained, and a rigid body model is presented. Then, the various forces acting on the system are described and modeled with proper assumptions. Followed by, the simulations showing the dynamic behaviour of estrogen docking into its receptor. Then the behaviour of estrogen when placed at different boundary conditions is analyzed highlighting the role played by the estrogen receptor in "locking" the docked estrogen. Then, the multi scale analysis is performed retaining the dynamics of the system while reducing the CPU run time up to 97%. Finally, the future scope for this work is presented laying the foundation for a new theoretical approach to screen the environmental chemicals.

APPENDIX A

Locations of bodies and points

Mass center of body A:

The masses of the atoms are available in Atomic Mass Unit (amu) (where $1amu = 1.66 \times 10^{-27}$ kilograms). From Table.A.1 and Fig.A.1, the mass of the body A is calculated and its value is *0.4323 Zg*.

The location of the center of mass (A_o) is calculated based on the center of mass for a system of particles as shown in Eq.A.1.

$$R = \frac{1}{M}\sum_{i=1}^{19} m_i r_i \tag{A.1}$$

where M - Mass of body A and r_i - Distance of m_i from the point from which the mass center is calculated, in this case, point A_1.

Table A.1: Masses used in model

Atom and Groups	Mass (Zg)
O	0.16
C	0.12
H	0.01
$-CH$	13.01
$-OH$	17.08
$-CH_2$	14.03
$-C_2H_3$	27

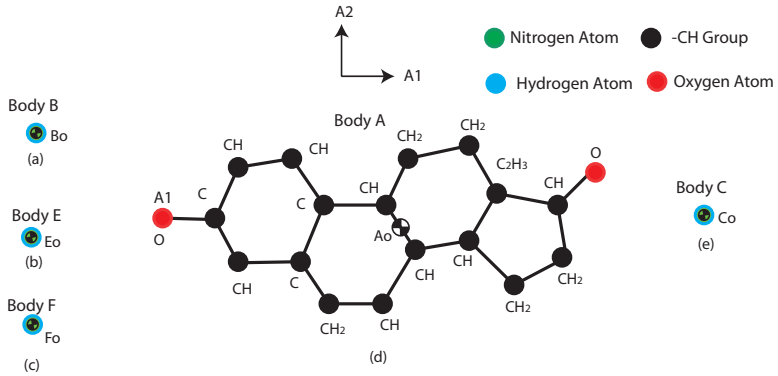

Figure A.1: The figure shows mass centers of the bodies used in this model

Locations of points in Coarse grained Estrogen:

The atom locations on the estogen are approximated from *3dchem.com* and that of the Estrogen receptor are calculated based on the stable bond lengths of the docked estrogen model obtained from the crystallographic studies on the docked estrogen [17].

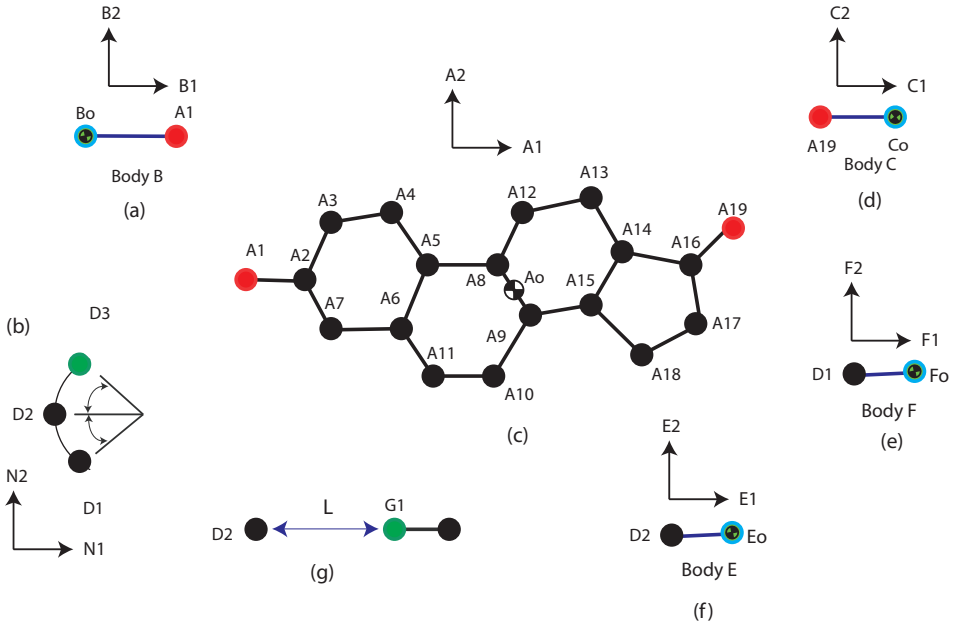

Figure A.2: The locations of coarse grained Estrogen

Table A.2: Locations of the bodies and points used in the model.

Point	from	Axis	
Body A		$A_1 >$	$A_2 >$
A1	A1	0	0
A_o	A1	6.2	0.48
A2	A1	1.38	0
A3	A1	2.08	1.2124
A4	A1	3.48	1.2124
A5	A1	4.2	0
A6	A1	3.48	-1.2421
A7	A1	2.08	-1.2124
A8	A1	5.7	0
A9	A1	6.4	-1.2124
A10	A1	5.7	-2.5
A11	A1	4.2	-2.5
A12	A1	6.4	1.325
A13	A1	7.92	1.325
A14	A1	8.66	0
A15	A1	7.92	-1.2124
A16	A1	10.26	-0.5983
A17	A1	10.26	-1.8107
A18	A1	8.8516	-2.4134
A19	A1	11.49	0.11
Body B		$B_1 >$	$B_2 >$
B_o	A1	-1	0
Body C		$C_1 >$	$C_2 >$
C_o	A19	1	0
Body E		$E_1 >$	$E_2 >$
E_o	D2	1	0
Body F		$F_1 >$	$F_2 >$
F_o	D1	1	0
D1, D2 and D3		$N_1 >$	$N_2 >$
D_2	N_o	0.5	0
D_1	D_2	2.5 $\cos(54^o)$	2.5 $\sin(54^o)$
D_3	D_2	1.86 $\cos(65^o)$	1.86 $\sin(65^o)$
Point G		$N_1 >$	$N_2 >$
G	D_2	19	0

APPENDIX B

Inertia Calculations

Inertia Calculation:

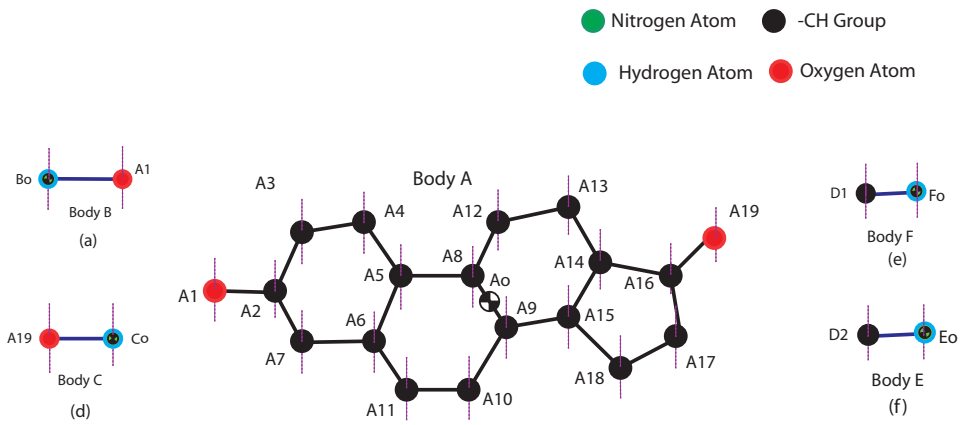

Figure B.1: Inertia calculation

The inertia of the system is calculated based on the following assumptions:

1. Each atom is assumed to be a solid sphere.
2. For the radius of the sphere: the *Covalent radius* of atoms is used.
3. At each points on body A where the $-CH$ groups are present, the radius of the sphere is assumed to be that of a Carbon atom, while the mass of the $-CH$ group is taken from Fig.A.1 and Table.A.1.

The inertia of the bodies is calculated about N_3 axis. For a solid sphere, the inertia (I_{33}) about N_3 is given by

$$I_{33} = \frac{2}{5} m r^2 \tag{B.1}$$

where m - mass of the atom; r - Covalent radii, see Table.B.1.

The inertia calculated about the body's own mass center is translated to the center of mass of body A (A_o) using the *parallel axis theorm*.

$$I_{A_o} = I_{33} + md^2 \tag{B.2}$$

Table B.1: Covalent Radii of individual atoms.

Atoms	Covalent radius ($\mathring{A}$)
C	0.73
H	0.31
O	0.66

where d is perpendicular distance between the two points.

For example, inertia calculation for A1:

$$I_{33,A_1} = \frac{2}{5} m_O {r_O}^2 \tag{B.3}$$

$$I_{33,A_O,A_1} = I_{33,A_1} + m_O d^2 \tag{B.4}$$

where m_O - Mass of Oxygen (See Tab.A.1), r_O - Covalent Radius of Oxygen (See Tab.B.1)

The inertia value thus calculated are summed up to get the final inertia of the body A about the N_3 axis, which is $0.3487 Zg - \mathring{A}^2$.

For the bodies B, C, E and F, the inertia is calculated using the above procedure about their respective joints as shown in Fig. 3.2.

APPENDIX C

Drag Forces

Table C.1: Rotational and Translational Drag coefficients calculated.

Atom	β_v	β_w
O	790.2	457
C	874	621
H	365.9	46.89

The calculated linear and rotational drag coefficients β_v and β_w respectively, for various atoms are shown in the Table.C.1.

However, for body A, to apply the viscous torque, it is assumed that the β_w for A is the sum of β_w for Oxygen, Hydrogen and Oxygen as shown in Tab.C.1.

APPENDIX D

Brownian Motion

Brownian Motion:

For the calculating the brownian motion , the value of β in Eq.D.1 are obtained from the Table.C.1.

$$E[B_{o1}^2(t)] = 2\beta k_B T = Var(C_{oi}(t)) = \sigma^2 \tag{D.1}$$

The values of k_B and T used in this model are 1.38×10^3 $(\frac{zg - \mathring{A}^2}{ns^2 K})$ and $300K$ respectively. The forces due to brownian motion are modeled by using β_v in Eq.D.1 and β_w is used in Eq.D.1 for modeling the torques on the atoms.

The Brownian motion is then applied on individual atoms. The Fig. D.1 shows the order of brownian force calculated for β_v of Oxygen from Eq.D.1.

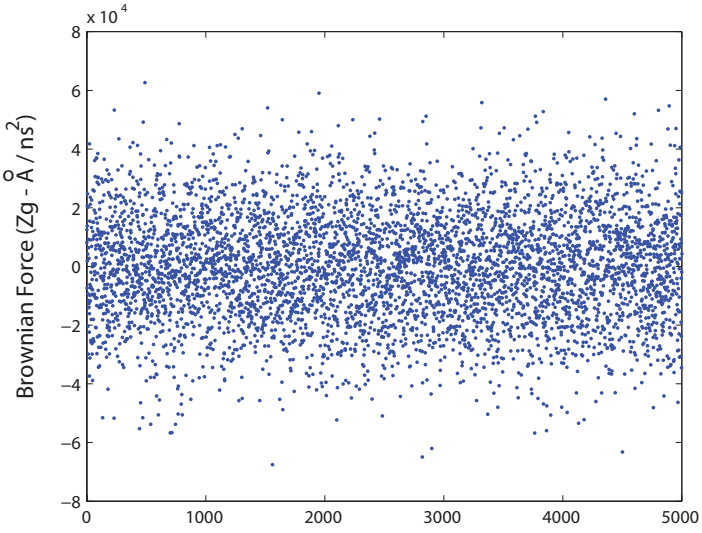

Figure D.1: Brownian Motion acting on Estrogen

REFERENCES

[1] P. Anand, A. B. Kunnumakara, C. Sundaram, K. B. Harikumar, S. T. Tharakan, B. S. Oiki S. Lai, and B. B. Aggarwal, "Cancer is a preventable disease that requires major lifestyle changes," *Pharmaceutical Research*, vol. 25, no. 9, p. 20972116, Sept. 2008.

[2] C. Theo, F. S. vom Saal, and A. M. Soto, "Developmental effects of endocrine-disrupting chemicals in wildlife and humans," *Environmental Health Perspectives*, vol. 101, pp. 378–384, 1993.

[3] G. P. Daston, J. W. Gooch, W. J. Breslin, D. L. Shuey, A. I. Nikiforov, T. A. F, and J. W. Gorsuch, "Environmental estrogens and reproductive health: A discussion of the human and environmental data," *Reproductive Toxicology*, vol. 11, no. 4, pp. 465–481, 1997.

[4] U. EPA, "Pesticide assessment guidelines, subdivision f, hazard evaluation: Human and domestic animals," NTIS Rpt., Tech. Rep. PB86-108958, 1984.

[5] R. M. Blair, H. Fang, W. S. Branham, B. S. Hass, S. L. Dia, C. L. Moland, W. Tong, L. Shi, R. Perkins, and D. M. Sheehan, "The estrogen receptor relative binding affinities of 188 natural and xenochemicals: Structural diversity of ligands," *Toxicological Sciences*, vol. 54, pp. 138–153, 2000.

[6] J. A. Katzenellenbogen, "The structural pervasiveness of estrogenic activity," *Environ Health Perspect*, vol. 103, no. 7, pp. 99–101, 1995.

[7] K. Fukuzawa, K. Kitaura, M. Uebayasi, K. Nakata, T. Kaminuma, and T. Nakano, "Ab initio quantum mechanical study of the binding energies of human estrogen receptor with its ligands: An application of fragment molecular

orbital method," *Journal of Computational Chemistry*, vol. 26, no. 1, p. 110, 2004.

[8] R. Bolger, T. E. Wiese, K. Ervin, S. Nestich, and W. Checovich, "Rapid screening of environmental chemicals for estrogen receptor binding capacity," *Environmental Health Perspectives*, vol. 106, no. 9, p. 137145, Sept. 1998.

[9] Asai.D and Shimohigashi.Y, "The assessment of xenoestrogens by competitive receptor binding assays," *Japanese Journal of Clinical Medicine*, vol. 58(12), pp. 2486–2490, 2000.

[10] *Guidance for Industry Safety Testing of Drug Metabolites*, U.S. Department of Health and Human Services, Food and Drug Administration, Center for Drug Evaluation and Research, February 2008.

[11] H. Fang, W. Tong, L. M. Shi, R. Blair, R. Perkins, W. Branham, B. S. Hass, Q. Xie, S. L. Dial, C. L. Moland, and D. M. Sheehan, "Structure-activity relationships for a large diverse set of natural, synthetic, and environmental estrogens," *Chemical Research in Toxicology*, vol. 14, pp. 280–294, 2001.

[12] G. N. Nikov, M. Eshete, R. V. Rajnarayanan, and W. L. Alworth, "Interactions of synthetic estrogens with human estrogen receptors," *Journal of Endocrinology*, vol. 170, p. 137145, 2001.

[13] A. M. Rossi and C. W. Taylor, "Analysis of protein-ligand interactions by fluorescence polarization," *Nature Protocols*, vol. 6, no. 3, pp. 365–387, 2011.

[14] K. Ohno, T. Fukushima, T. Santa, N. Waizumi, H. Tokuyama, M. Maeda, and K. Imai, "Estrogen receptor binding assay method for endocrine disruptors using fluorescence polarization," *Analytical Chemistry*, vol. 74, pp. 4391–4396, 2002.

[15] J. Payne, M. Scholze, and A. Kortenkamp, "Mixtures of four organochlorines enhance human breast cancer cell proliferation," *Environmental Health Perspectives*, vol. 109, no. 4, pp. 391–397, 2001.

[16] G. D. Charles, C. Gennings, T. R. Zacharewski, B. B. Gollapud, and E. W. Carney, "An approach for assessing estrogen receptor-mediated interactions in mixtures of three chemicals: A pilot study," *Toxicological Sciences*, vol. 68, pp. 349–360, 2002.

[17] N. Heldring, A. Pike, S. Andersson, J. Matthews, G. Cheng, J. Hartman, M. Tujague, A. StroM, E. Treuter, M. Warner, and J.-A. K. Gustafsson, "Estrogen receptors: How do they signal and what are their targets," *Physiol Rev*, vol. 87, p. 905931, 2007.

[18] P. Hu, H. K. Kinyamu, L. Wang, J. Martin, T. K. Archer, and C. Teng, "Estrogen induces estrogen-related receptor alpha gene expression and chromatin structural changes in estrogen receptor (er)-positive and er-negative breast cancer cells," *The Journal of Biological Chemistry*, vol. 283, no. 11, p. 67526763, 2008.

[19] R. Metivier, A. Stark, G. Flouriot, M. R. Hubner, H. Brand, G. Penot, D. Manu, S. Denger, G. Reid, M. Kos, R. B.Russell, O. Kah, F. Pakdel, and F. Gannon, "A dynamic structural model for estrogen receptor - activation by ligands, emphasizing the role of interactions between distant a and e domains," *Molecular Cell*, vol. 10, p. 10191032, Nov. 2002.

[20] M. Ruff, M. Gangloff, J. M. Wurtz, and D. Moras, "Estrogen receptor transcription and transactivation structurefunction relationship in dna- and ligand-binding domains of estrogen receptors," *Breast Cancer Research*, vol. 2, pp. 353–359, 2000.

[21] D. M. Tanenbaum, Y. Wang, S. P. Williams, and P. B. Sigler, "Crystallographic comparison of the estrogen and progesterone receptors ligand binding domains," *Proceedings at National Academy of Science USA*, vol. 95, p. 59986003, May 1998.

[22] A. M. Brzozowski, A. C. W. Pike, Z. Dauter, R. E. Hubbard, T. Bonn, O. Engstro, L. O. hman, G. L. Greene, J.-A. Gustafsson, and M. Carlquist, "Molecular basis of agonism and antagonismin the estrogen receptor," *Nature*, vol. 389, pp. 753 – 758, Oct. 1997.

[23] M. Karplus and G. A.Petsko, "Molecular dynamics simulations in biology," *Nature*, vol. 347, pp. 631–639, 1990.

[24] L. Celik, J. D. D. Lund, and B. Schiott, "Conformational dynamics of the estrogen receptor r: Molecular dynamics simulations of the influence of binding site structure on protein dynamics," *Biochemistry*, vol. 46, pp. 1743–1758, 2006.

[25] A. A. Pinkerton, "Measurement of the electron density distribution of estrogens-a first step to advance drug design," The University of Toledo, Toledo, Ohio, Tech. Rep., August 2001.

[26] E. A. Zhurova, C. F. Matta, N. Wu, V. V. Zhurov, and A. A. Pinkerton, "Experimental and theoretical electron density study of estrone," *Journal of American Chemical Society*, vol. 128, no. 27, pp. 8849–8861, 2006.

[27] D. Parrish, E. A. Zhurova, K. Kirschbaum, and A. A. Pinkerton, "Experimental charge density study of estrogens: 17 beta-estradiol.urea," *Journal of Physical Chemistry*, vol. 110, no. 51, pp. 26 442–26 447, 2006.

[28] E. A. Zhurova, V. V. Zhurov, D. Chopra, A. I. Stash, and A. A. Pinkerton, "17 alpha-estradiol.1/2 h2o: Super-structural ordering, electronic properties, chemical bonding, and biological activity in comparison with other estrogens," *Journal of American Chemical Society*, vol. 131, p. 1726017269, 2009.

[29] K. Fukuzawa, Y. Mochizuki, S. Tanaka, K. Kitaura, and T. Nakano, "Molecular interactions between estrogen receptor and its ligand studied by the ab initio fragment molecular orbital method," *Journal of Physical Chemistry*, vol. 110, pp. 16 102–16 110, 2006.

[30] C. Watanabe, K. Fukuzawa, Y. Okiyama, T. Tsukamoto, A. Kato, S. Tanaka, T. Nakano, and Y. Mochizuki, "New fragmentation of fragment molecular orbital method applicable to fragment based drug design," 2012, this article speaks of Fragment Molecular Orbital (FMO) approach applicable to Fragment Based Drug Design, uses the Inter-fragment interaction energy (IFIE) analysis based on the ab initio fragment molecular orbital (FMO) method to revealed ligand binding mechanism of the ER.

[31] B. R. Brooks, C. L. B. III, A. D. M. Jr., L. Nilsson, R. J. Petrella, B. Roux, Y. Won, G. Archontis, C. Bartels, S. Boresch, A. Caflisch, L. Caves, Q. Cui, A. R. Dinne, M. Feig, S. Fischer, J. Gao, M. Hodoscek, W. Im, K. Kuczera, T. Lazaridis, J. Ma, V. Ovchinnikov, E. Paci, R. W. Pastor, C. B. Post, J. Z. Pu, M. Schaffer, B. Tidor, R. M. Venable, H. L. Woodcock, X. Wu, W. Yang, D. M. York, and M. Karplus, "Charmm: The biomolecular simulation program," *Journal of Computational Chemistry*, vol. 30, no. 10, pp. 1545–1614, 2009.

[32] S. J. Yu, S. M. Keenan, W. Tong, and W. J. Welsh, "Influence of the structural diversity of data sets on the statistical quality of three-dimensional quantitative structure-activity relationship (3d-qsar) models: Predicting the estrogenic activity of xenoestrogens," *Chemical Research in Toxicology*, vol. 15, pp. 1229–1234, 2002.

[33] M. Poursina and K. S. Anderson, "Canonical ensemble simulation of biopolymers using a coarse-grained articulated generalized divide-and-conquer scheme," *Computer Physics Communications*, vol. 184, no. 3, pp. 652–660, 3 2013.

[34] M. Haghshenas-Jaryani and A. Bowling, "Multiscale dynamic modeling of flexibility in myosin v using a planar mechanical model," in *Proceedings of the IEEE International Conference Robotics and Biomimetics (ROBIO)*, December 11-14 2012.

[35] J. C. Chen and A. S. Kim, "Brownian dynamics, molecular dynamics, and monte carlo modeling of colloidal systems," *Advances in Colloid and Interface Science*, vol. 112, no. 1-3, pp. 159–173, December 2004.

[36] A. Ciudad, J. M. Sancho, and G. P. Tsironis, "Kinesin as an electrostatic machine," vol. 32, no. 5, pp. 455–463, November 2006.

[37] F. Reif, *Fundamentals of Statistical and Thermal Physics*. McGraw Hill New York, 1965.

[38] J. Yu, T. Ha, and K. Schulten, "Structure-based model of the stepping motor of PcrA helicase," *Biophysical Journal*, vol. 91, no. 6, pp. 2097–2114, September 2006.

[39] H. Rafii-Tabar, Y. Jamali, and A. Lohrasebi, "Computational modelling of the stochastic dynamics of kinesin biomolecular motors," *Physica A*, vol. 381, pp. 239–254, July 2007.

[40] K. B. Zeldovich, J. F. Joanny, and J. Prost, "Motor proteins transporting cargos," *European Physical Journal E*, vol. 17, no. 2, pp. 155–163, June 2005.

[41] H. Wang and T. C. Elston, "Mathematical and computational methods for studying energy transduction in protein motors," *Journal of Statistical Physics*, vol. 128, no. 1-2, pp. 35–76, July 2007.

[42] E. Cunningham, "On the velocity of steady fall of spherical particles through fluid medium," *Proceedings of Royal Society London*, vol. 83, pp. 357–365, March 1910.

[43] G. Ahmadi, "Hydrodynamic forces, drag force and drag coefficient," Course Material for ME437/537.

[44] J. N. Israelachvili, *Intermolecular and Surface Forces*, 2nd ed. Academic Press, 2002.

[45] A. Bowling, A. F. Palmer, and L. Wilhelm, "Contact and impact in the multibody dynamics of motor protein locomotion," *Langmuir*, vol. 25, no. 22, pp. 12 974–12 981, Nov. 2009. [Online]. Available: http://pubs.acs.org/toc/langd5/0/0

[46] K. Hayashi and M. Takano, "Violation of the fluctuation-dissipation theorem in a protein system," *Biophysical Journal*, vol. 93, no. 3, pp. 895–901, August 2007.

[47] M. Haghshenas-Jaryani, J. Drake, N. Tran, A. Bowling, and S. Mohanty, "Multi-scale modeling and simulation of a microbead in an optical trapping process," in *Proceedings of the ASME 2nd Global Congress on Nanoengineering for Medicine and Biology (NEMB2013)*, February 4-6 2013.

[48] M. Haghshenas-Jaryani and A. Bowling, "Multiscale dynamic modeling of processive motor proteins," in *Proceedings of the IEEE International Conference Robotics and Biomimetics (ROBIO)*, December 7-11 2011, pp. 1403–1408.

BIOGRAPHICAL STATEMENT

Anudeep Palanki was born in Visakhapatnam, India in 1990. He received his Bachelors in Technology (B.Tech.) degree in Mechanical Engineering from Jawaharlal Nehru Technological University, Kakinada, India, in 2011. He recieved his M.S. degree, also in Mechanical Engineering from The University of Texas at Arlington in 2013. His current research interest is in the area of Robotics and Biomechanics. He is a member of ASME.